# Measurement and Numerical Analysis on Deformation of Natural Rock Slope under Temperature Variation

Mufundirwa Azania[1] and Fujii Yoshiaki[1]
[1]Laboratory of Rock Mechanics, Hokkaido University, Sapporo, Japan

**Abstract:** A 767-day long displacement and temperature record for a natural rock slope in Iwate prefecture (Shimohei district, Kawai village) in Japan was monitored. The natural rock slope, poses as an existing potential failure that may cause disaster if rock falls occur. Six surface crack displacement sensors (ch1–ch6) were installed on surface of natural rock slope. Displacements were mainly due to thermal strains and only ch1 gave a steep opening of fracture. Numerically, the behaviour of rock slope with a one-meter deep fracture under temperature variation was analysed using a (5 m × 5 m) two-dimensional plane strained, confined and unconfined models using elastic and elasto-plastic finite element analysis. Generally, in elastic and elasto-plastic conditions, fracture closed with temperature raising and vice-versa. Expansion of rock mass due to freezing at sub-zero temperatures was observed. Large tensile stresses appear at the fracture tip when temperature lowered, thus generating tensile failure and a small increase in fracture opening under elasto-plastic conditions in confined cases only.

**Keywords:** Natural Rock slope; Displacement; Temperature; Numerical analysis

## Introduction

Potential rock slope failures are a major threat if they are located near a roadway or a railway. In Japan, some fatal accidents have occurred in the past due to large-scale slope collapse on roads and railways, disrupting transportation and normal daily activities [1-2]. Consequently, ensuring the stability of rock slopes is a major priority. Continuous monitoring through field measurements is vital to assess slope stability during the service life [3]. In cold regions, rock falls are normally reported in early spring due to thawing of snow.

In this study, a 767-day long displacement and temperature record for a natural rock slope in Iwate prefecture (Shimohei district, Kawai village) in Japan is described. The natural rock slope, poses as an existing potential failure that may cause train accident if rock falls occur. Six surface fracture displacement sensors (ch1–ch6) were installed on the surface of natural rock slope for continuous measurement of rock slope deformations.

Numerically, the behaviour of rock slope with a one-meter deep fracture under temperature variations was analysed using a (5 m × 5 m) two-dimensional plane strained, confined and unconfined models using elastic and elasto-plastic finite element analysis (FEM). Important deformation characteristics were deduced from the field measurements and numerical results.

## Site

The natural rock slope is located in Iwate prefecture, Japan. Geology of the rock slope consisted of chert block with some slates. Six surface fracture displacement sensors were installed on the surface of natural rock slope as shown in Figure 1. The displacement sensors (Kyowa, BCD-5B model) had an operating range of −10 to 60°C, ±5 mm measuring range, and a rated output of ±1 mV/V (2000 × $10^{-6}$). Weather conditions namely, air temperature, humidity, snowfall, and rainfall were recorded from 9 November 2006 to 14 December 2008 (Figure 1).

## Measured Trends

Variations of air temperature ($T_a$) and fracture displacement ($u$) on the natural rock slope for each channel are as shown in Figure 2. Generally, rock mass expands or shrinks with temperature variation. Maximum and minimum temperatures achieved were 23°C and −4.1°C, respectively. Roughly, temperature-induced displacement varied sinusoidally with temperature, that is, thermal expansion or thermal contraction. This means other displacements that occur, may be due to external factors or processes affecting movement of the fracture or rock mass.

For ch1, at $t$ = 286 days fracture or rock mass moved (ch1 in Figure 2). It occurred during the summer period on 21 August 2007 at 23:00. A nearly sharp vertical displacement of 0.22 mm was recorded, that moved from −0.18 mm to 0.04 mm at temperatures of 22.4°C and 22.7°C, respectively. This displacement was not temperature-induced. There was little rain (0.2 mm/day) and humidity was high at 89.1%. Fracture displacement sensor, ch2, was installed on highly fractured rock mass (Figure 1). It gave variations of displacement that were significantly different from all the other channels (ch2 in Figure 2). Ch4 and ch6 reflect some permanent deformations of 0.13 mm and 0.19 mm, respectively (Figure 2).

However, for ch2–ch6, no significant displacements due to external processes affecting the fracture or rock mass were observed. The recorded displacement data contains temperature-induced

displacements due to thermal expansion or contraction. Therefore, attempts to minimise these displacements were done.

**Corrected Displacements**

To minimise displacements due to thermal expansion or contraction, Eq. (1) was used.

$$u' = u + AT_a \quad (1)$$

$$U_a = u'_{max} - u'_{min} \quad (2)$$

where $u'$ is the corrected displacement, $u$ is displacement (moving averaged), $A$ is correction coefficient, $T_a$ is air temperature (moving averaged), $U_a$ is displacement amplitude, $u'_{max}$ is maximum displacement, and $u'_{min}$ is minimum displacement.

Different correction coefficients, $A$, were analysed. The correction coefficient, $A$, that gave the lowest or minimum displacement amplitude was used to correct the displacement. Correction coefficients range is +0.005 mm/K to +0.007 mm/K, except for ch2. The correction coefficient for ch2 is −0.003 mm/K, which is very different from other channels. This may possibly be due to the highly fractured nature of rock mass within the vicinity of ch2 as shown in Figure 1.

For ch1 under corrected displacements, at $t \approx 40$ weeks, equivalent to 23:00 August 21, 2007, a steep increase in displacement of 0.22 mm was also observed (ch1 in Figure 3). This may possibly be due to fracture or rock mass movement again, as in ch1 in Figure 2, for measured displacements. Displacement sensor ch1 had a correction coefficient of +0.007 mm/K.

Displacement sensor, ch2 had a correction coefficient of −0.003 mm/K. At ch2, fracture tends to open and close with temperature increase and decrease, respectively with some lag (ch2 in Figure 3). Ch3 had a correction coefficient of +0.007 mm/K. Displacement variations are very small, and the possibility of fracture propagation is very low. Ch4 had a correction coefficient of +0.005 mm/K. The fracture is gradually opening, and the possibility of fracture propagation is high (ch4 in Figure 3). Ch5 had a correction coefficient of +0.006 mm/K. Very small displacement variations are observed (ch5 in Figure 3). For ch6, fracture was generally closing (ch6 in Figure 3). The correction coefficient was +0.005 mm/K. Permanent deformations were observed in all the channels from 0.03–0.21mm (Figure 3).

**Numerical Analysis**

Numerically, the behaviour of rock slope with a one-meter deep fracture under temperature variation was analysed using a (5 m × 5 m) two-dimensional plane strained model. Two boundary conditions were used; confined and unconfined conditions under elastic and elasto-plastic finite element analysis as shown in Figure 4. Two patterns of transient heat analysis (variable temperature boundary) were conducted on the rock surface in confined and unconfined conditions. The first temperature pattern had a positive temperature variation (7.8–32.2°C), with an initial temperature of 20°C applied as the temperature of rock mass. The second temperature pattern had positive and sub-zero temperatures (–2.2–22.2°C), with an initial temperature of 10°C applied as the temperature of rock mass.

**Analytical model**

A 2-D finite element mesh was generated (864 elements, 467 nodes). The thermal displacement in the $x$-direction ($u_x$) was calculated by considering nodal displacements of the fracture at the rock surface (node 442) as shown in Figure 4a and b. The model is symmetrical about the $y$-axis, and tensile stresses are taken as positive (+) and compressive stresses as negative (–) in this numerical analysis. Positive displacements means fracture opening and negative displacements means fracture closure.

**Analytic conditions**

A total of 8 numerical simulations were performed. These were elastic and elasto-plastic analysis under the two transient temperature patterns. These are:

(1) Elastic model under confined boundary conditions;
(2) Elastic model under unconfined boundary conditions;
(3) Elasto-plastic model under confined boundary conditions; and
(4) Elasto-plastic model under unconfined boundary conditions.

The rock mass is assumed to be homogeneous and isotropic.

**Analytic results and discussion**

Thermal displacements under elastic and elasto-plastic analysis were calculated. The stability of the natural rock slope was then assessed by analysing displacement from numerical simulations and measured results. The properties of rock used in the FEM analysis are as in Table. 1.

**Elastic conditions**

(a) Elastic-confined conditions under positive temperature (7.8–32.2°C) were done as shown in Figure 5. As temperature increased, the rock mass expanded, i.e. at maximum temperature 32.2°C, the rock mass expanded as shown in Figure 5a. As the rock mass expanded, the fracture closed. At the fracture tip, compressive stresses were observed

($-\sigma_x < q_u$), therefore no compressive failure was observed (Figure 5b). As temperature decreased, the rock mass contracted, i.e. at minimum temperature 7.8°C, rock mass contracted as illustrated in Figure 5c, thereby causing the fracture to open. Large tensile stresses around 30.8 MPa ($\sigma_x > T_o$) at the fracture tip were observed (Figure 5d). This condition may lead to fracture propagation, thereby deepening the fracture into the rock mass. Displacement is almost linear with temperature. However, corrected displacement looks like inelastic and irrecoverable although the model is completely elastic. This is because heat transmission requires some time.

(b) Elastic-unconfined conditions under positive temperature (7.8–32.2°C) were done. At maximum temperature 32.2°C, rock mass expanded. Expansion of rock mass along the fracture length practically means the fracture closure. At the fracture tip, very small compressive stresses were observed ($-\sigma_x < q_u$), therefore no compressive failure was observed. At minimum temperature of 7.8 °C, there were small tensile stresses ($\sigma_x < T_o$) compared to those under elastic-confined conditions. No fracture propagation is likely to occur, hence the rock slope is in a stable condition. Displacement looks like inelastic and irrecoverable particularly in corrected displacement.

(c) Elastic-confined conditions under positive and sub-zero temperatures (–2.2–22.2°C) were analysed. At maximum temperature 22.2°C, similar compressive stresses were observed around the fracture tip as in elastic-confined under positive temperature only (Figure 5b). No compressive failure in the rock mass was observed. At minimum temperature –2.2°C, large tensile stresses ($\sigma_x > T_o$) were observed around the fracture tip. These conditions trigger fracture propagation. The tensile stresses generated at minimum temperature are smaller than those in Figure 5d. This is due to expansion of rock mass as a result of freezing of pore water at sub-zero temperatures, which led to fracture closure, hence resulting in small tensile stresses around fracture tip.

(d) Elastic-unconfined conditions under positive and sub-zero temperatures (–2.2–22.2°C) were conducted. At maximum temperature 22.2°C, similar distributions of compressive stresses were observed. At minimum temperature –2.2°C, lowest tensile stresses ($\sigma_x < T_o$) were generated. Therefore, no fracture propagation is likely to occur. Very small displacements of fracture closure due to freezing were observed.

**Elasto-plastic conditions**

(a) Elasto-plastic confined conditions under positive temperature (7.8–32.2°C) were done as shown in Figure 6. At maximum temperature 32.2°C, similar results were obtained as in Figure 5a and b. At the fracture tip, compressive stresses were observed ($-\sigma_x < q_u$), therefore no compressive failure was observed and there was no element failure as shown in Fig. 6e. At minimum temperature 7.8°C, there was tensile failure of 6 elements around fracture tip (Figure 6f). A small increase in displacement is observed from $t$ = 33–42 weeks as temperature decreased to minimum levels (Figure 8a). Displacement gradually returned back towards zero as temperature started to increase from $t$ = 43–52 weeks (Figure 8a).

(b) Elasto-plastic confined conditions under positive and sub-zero temperature (–2.2–22.2°C) were done as shown in Figure 7. At minimum temperature –2.2°C, large tensile stresses ($\sigma_x > T_o$) resulted in tensile failure of four elements around fracture tip (Figure 7f). A small increase in displacement is observed from $t$ = 33–45 weeks as temperature decreased to minimum levels in the sub-zero range (Figure 8b). Displacement gradually returned back towards zero as temperature started to increase above 0°C from $t$ = 46–52 weeks (Figure 8b).

(c) Elasto-plastic unconfined conditions under both temperature variations were carried out. There was no element failure.

**Concluding remarks**

There have been relatively fatal train accidents that occurred in Japan in past years due to rock falls landing on railway lines in cases where a rock slope is adjacent to railway line. Therefore, rock slope deformations arising from thermal stresses have been predicted using 2-D finite element analysis. Analysis of the measured and calculated displacement provided an understanding of the deformations on the natural rock slope.

Measured displacement results and numerical results showed closing of fracture as temperature increased and vice-versa for all the channels, except for ch2. This may be attributed to difference in rock mass structure and installations conditions. Rock mass in the vicinity of ch2 was highly fractured. Attempts to minimise displacement due to thermal expansion or contraction were done. In corrected displacement, ch1 also gave a clear fracture or rock mass movement. Channels, Chs3 and 4, exhibit very small temperature-induced fracture displacements ≈ 0.01 mm over a period of over two years. Ch5 was gradually opening whilst Ch6 was generally closing. Generally, no significant weather conditions on fracture or rock mass movement were observed.

A 2-D finite element model was generated to earn basic knowledge of the behaviour of rock slope with fractures under temperature variation. Elastic and elasto-plastic analysis was done. Behaviour of the fracture in confined and unconfined boundary

conditions was analysed. It is concluded that, under elastic and elasto-plastic conditions:

- Fracture closed as temperature increased and vice-versa under both temperature variations.
- Displacement was larger in confined conditions as compared to unconfined conditions.
- Tensile stress appeared at the fracture tip when temperature lowered.
- Compressive stress appeared at the fracture tip when temperature was raised.
- Under sub-zero temperature, in confined conditions, displacement caused by expansion due to freezing is much larger than in unconfined conditions.

In elasto-plastic conditions:

- Under both temperature variations, in unconfined conditions, there was no fracture propagation at maximum and minimum temperatures.
- Under both temperature variations, in confined conditions, there was fracture propagation at minimum temperatures of 7.8°C and –2.2°C, respectively. At 7.8°C, there was generation of a wider tensile failure region as compared to that at –2.2°C. This is because, at sub-zero temperatures –2.2°C, the fracture tends to close due to expansion of rock mass as a result of freezing, thus generating lower tensile stresses hence the resulting smaller tensile region.
- Thermal displacements under elasto-plastic analysis were slightly larger than those in elastic analysis as temperature lowered under confined boundary conditions as shown by dotted lines (Figure 8).
- Corrected displacement show expansion due to freezing more clearly.

It was realized that non-linear deformations do not have to represent fracture propagation through numerical analysis. The results would also suggest that freezing effects on deformation of rock slope are not so significant. However, effects of freezing should be further investigated.

**References**

[1] Saito M. 1969, Forecasting time of slope failure by tertiary creep. In: Proceedings of seventh international conference on soil mechanics and foundation engineering, Mexico City, 2. p677-683.

[2] Shiotani T. Evaluation of rock stability by means of acoustic emission. Int Conference on Emerging Technologies in Non-Destructive Testing, Keynote lecture, Greece, 2003.

[3] Rose ND, Hungr O. Forecasting potential rock slope failure in open pit mines using the inverse-velocity method. Int J Rock Mech Min Sci 2007; 44:308-20.

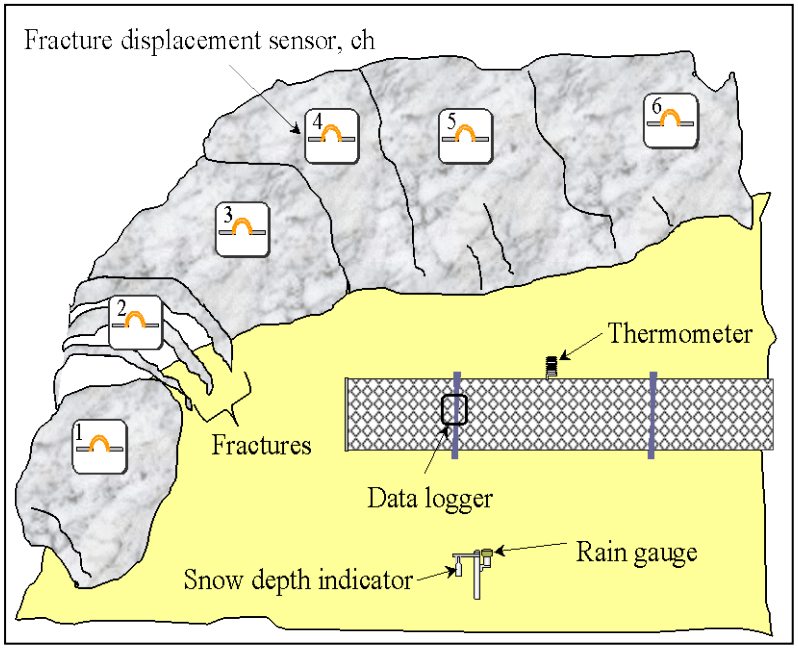


Figure 1. Schematic diagram of natural rock slope showing layout of fracture displacement sensors and weather measuring equipment.

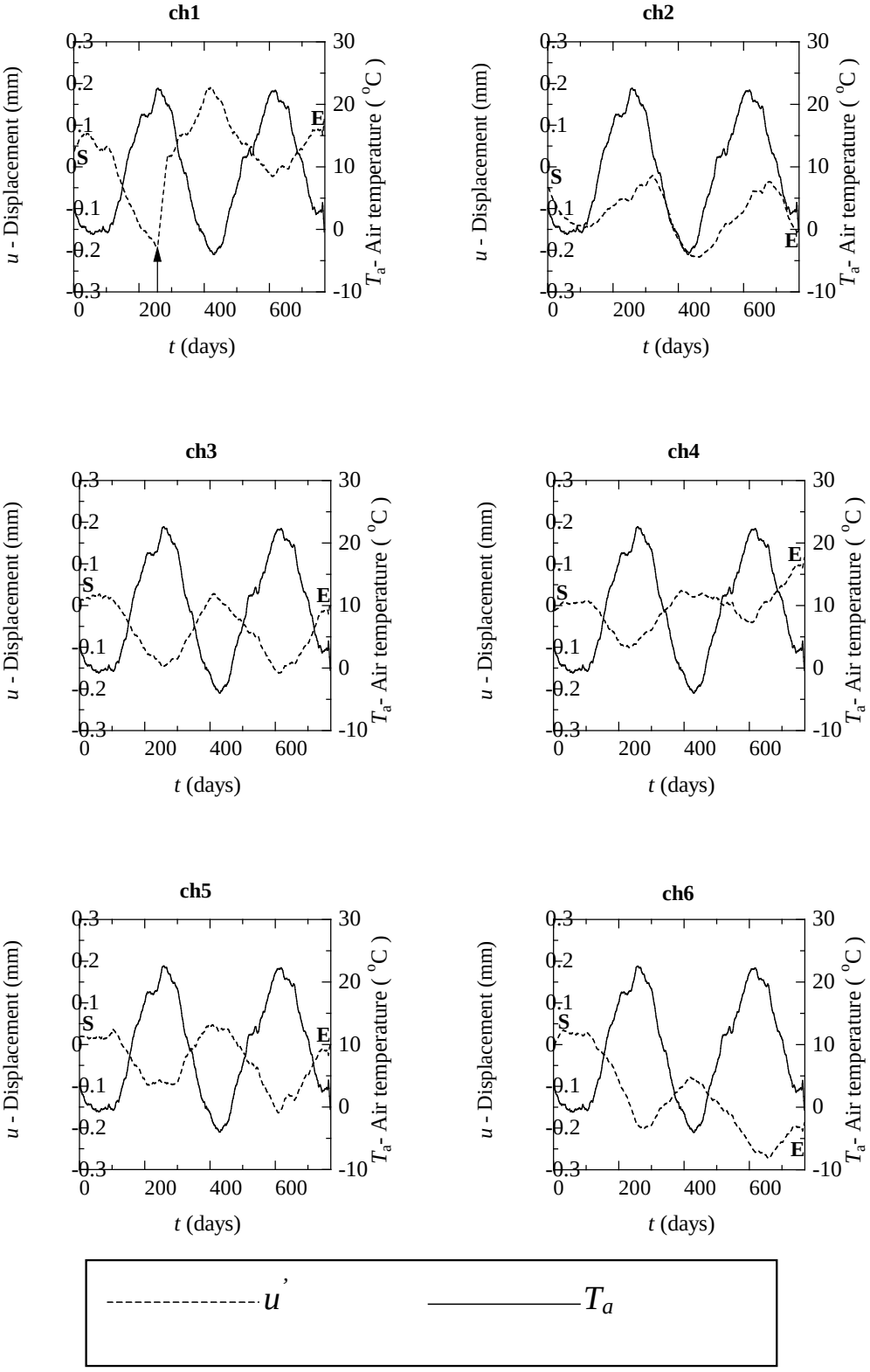


Figure 2. Variations of air temperature $T_a$ (one-day average) and displacement $u$ (one-day average) against time $t$ for six surface fracture displacement sensors, ch1–ch6. Note: **S** and **E** denote the start and end of monitored displacement.

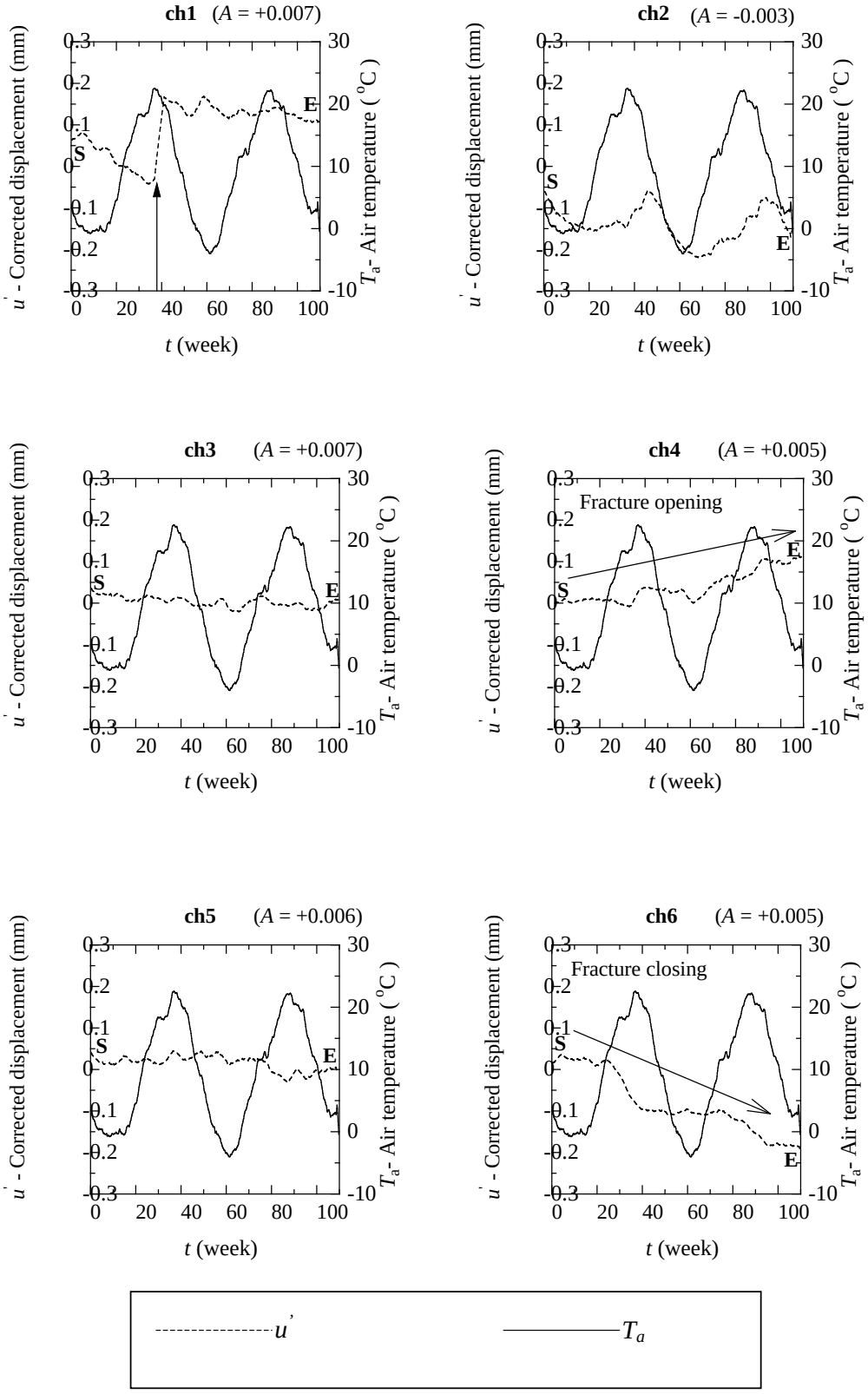


Figure 3. Variations of air temperature $T_a$ (moving averaged) and corrected displacement $u'$ (moving averaged) against time $t$ for six surface fracture displacement sensors, ch1–ch6. Note: **S** and **E** denote the start and end of monitored displacement.

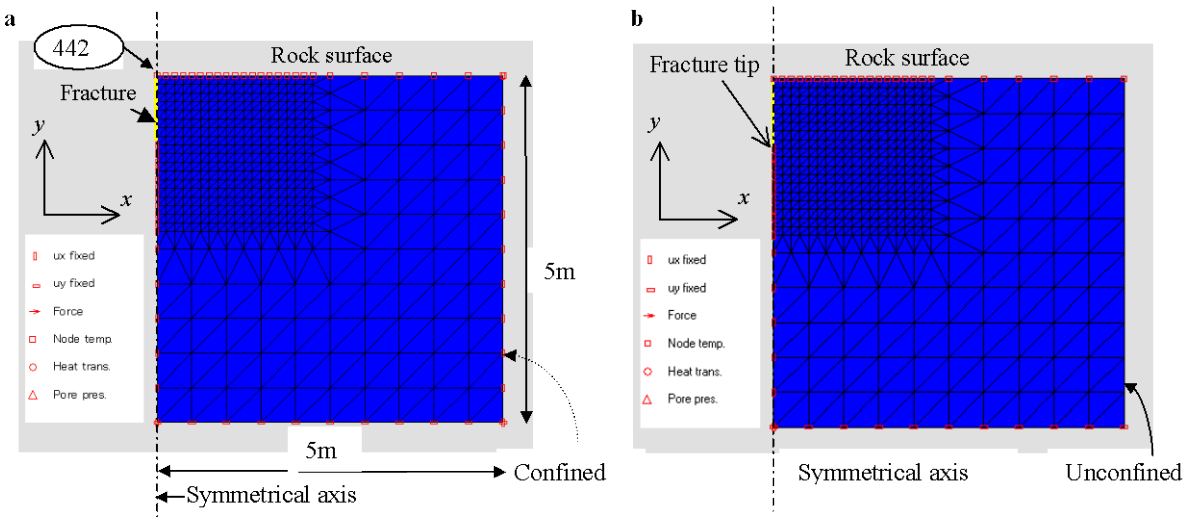


Figure 4. Finite element models: (a) Confined, (b) Unconfined. Note: 442 is node number that represents the beginning of the fracture at the rock surface. The fracture has some aperture.

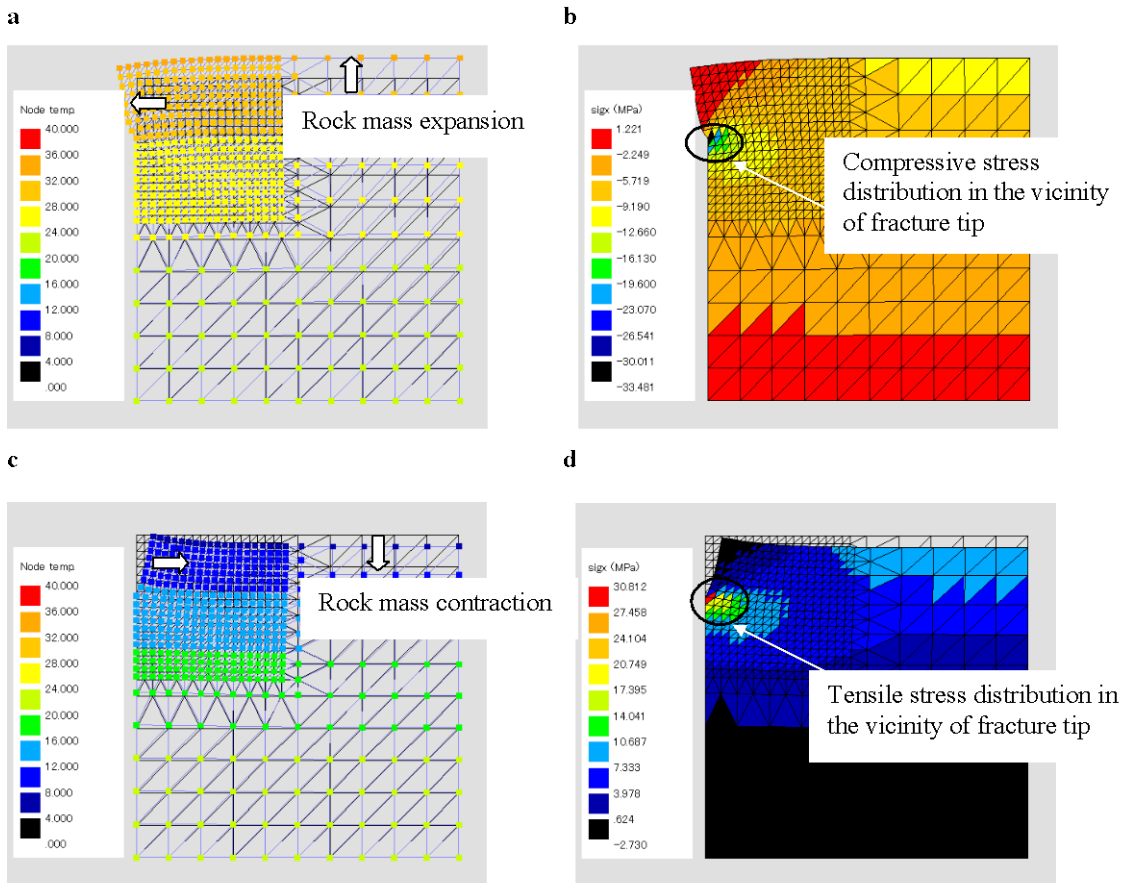


Figure 5. Calculated results of Elastic-confined FEM model: (a) Temperature distribution in rock mass at maximum temperature, 32.2°C, (b) Stress in *x*-direction $\sigma_x$ at 32.2°C, (c) Temperature distribution in rock mass at minimum temperature, 7.8 °C, and (d) Stress in *x*-direction $\sigma_x$ at 7.8°C. Note: Deformation is magnified × 1000.

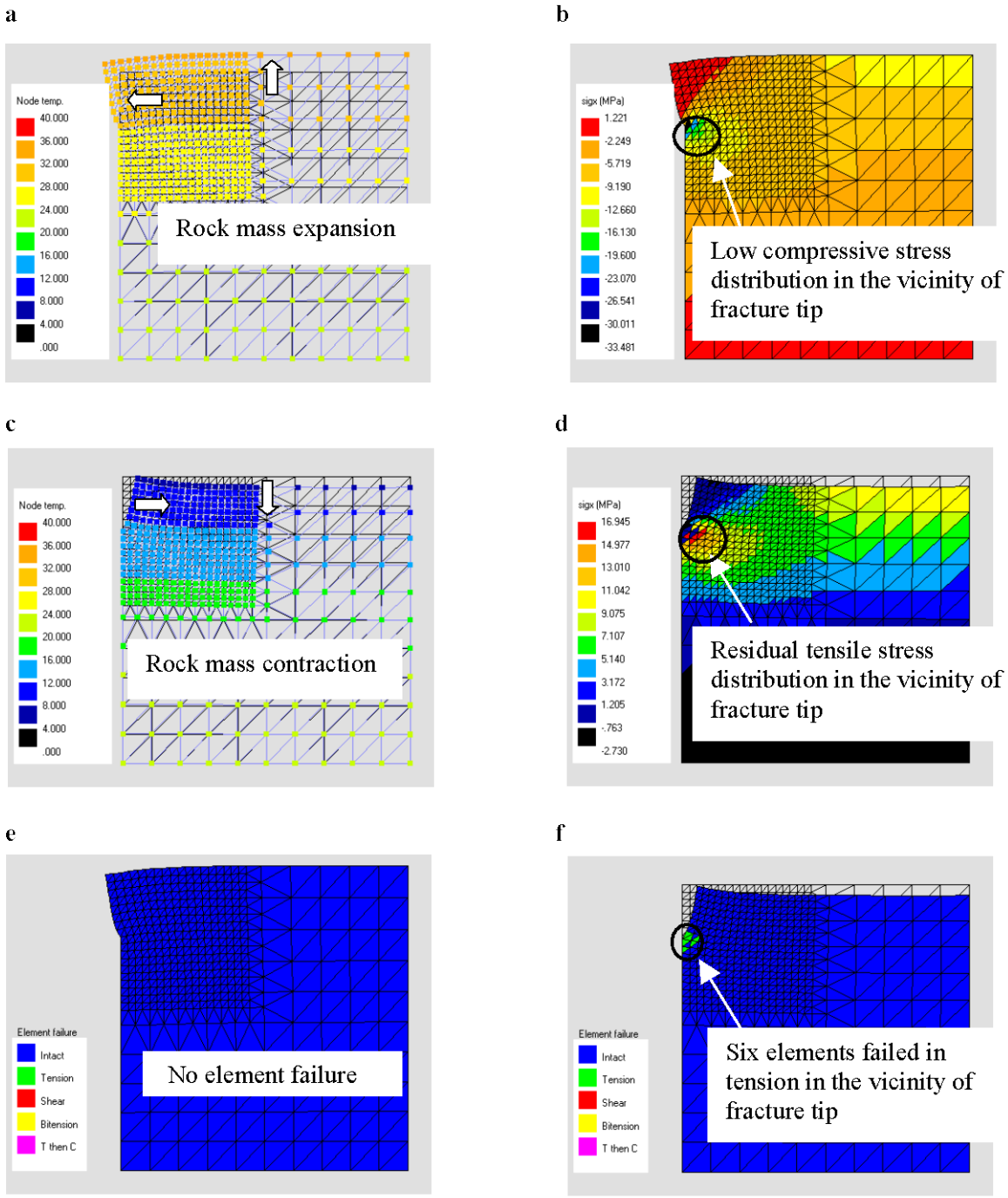


Figure 6. Calculated results of Elasto-plastic confined FEM model: (a) Temperature distribution in rock mass at maximum temperature 32.2°C, (b) Stress in *x*-direction $\sigma_x$ at 32.2°C, (c) Temperature distribution in rock mass at minimum temperature 7.8°C, (d) Stress in *x*-direction $\sigma_x$ at 7.8 °C, (e) Element failure at maximum temperature, 32.2°C, and (f) Element failure at minimum temperature 7.8°C. Note: Deformation is magnified $\times$ 1000.

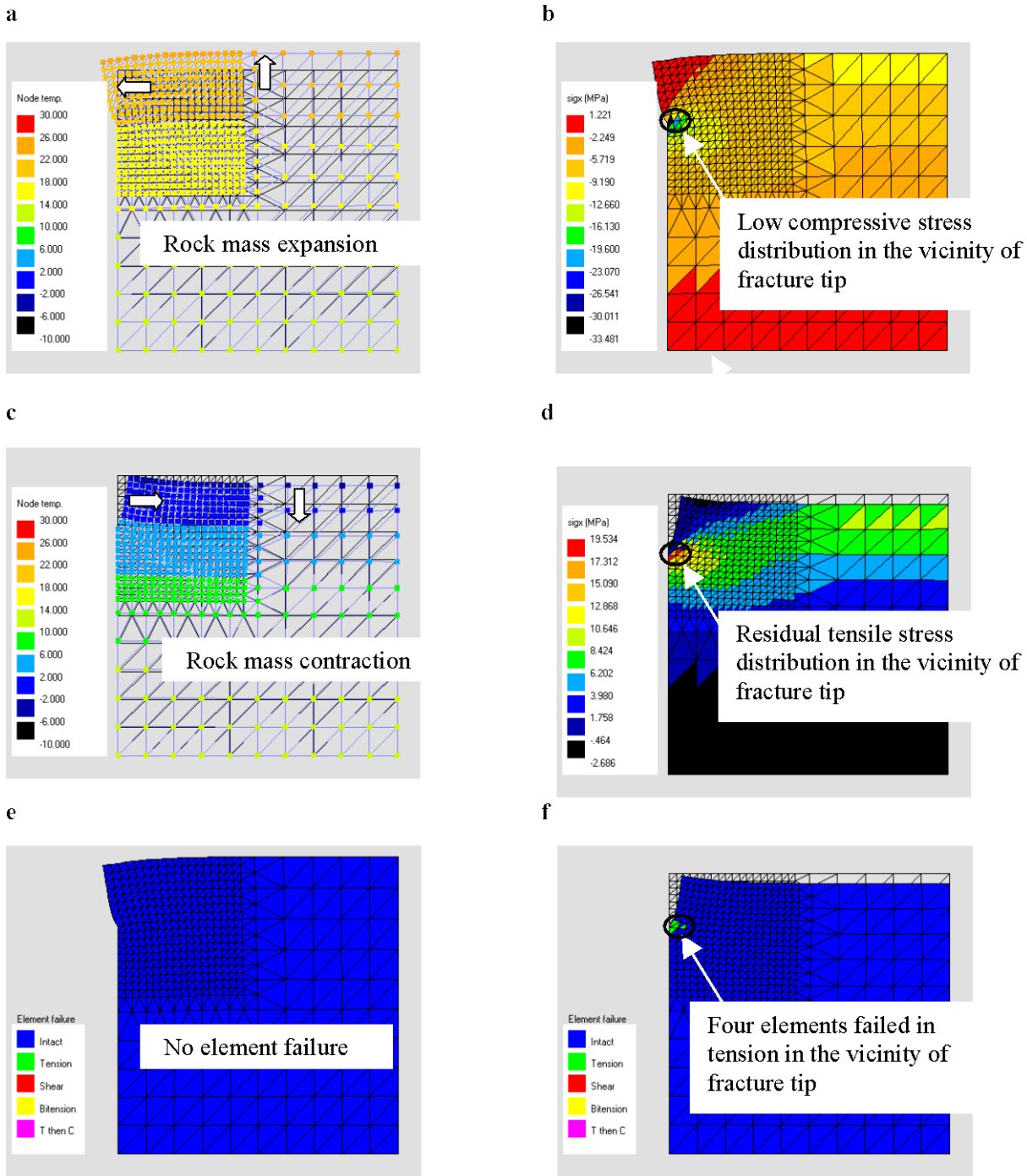


Figure 7. Calculated results of Elasto-plastic confined FEM model: (a) Temperature distribution in rock mass at maximum temperature 22.2°C, (b) Stress in *x*-direction $\sigma_x$ at 22.2°C, (c) Temperature distribution in rock mass at minimum temperature –2.2°C, (d) Stress in *x*-direction $\sigma_x$ at –2.2°C, (e) Element failure at maximum temperature, 22.2°C, and (f) Element failure at minimum temperature –2.2°C. Note: Deformation is magnified × 1000.

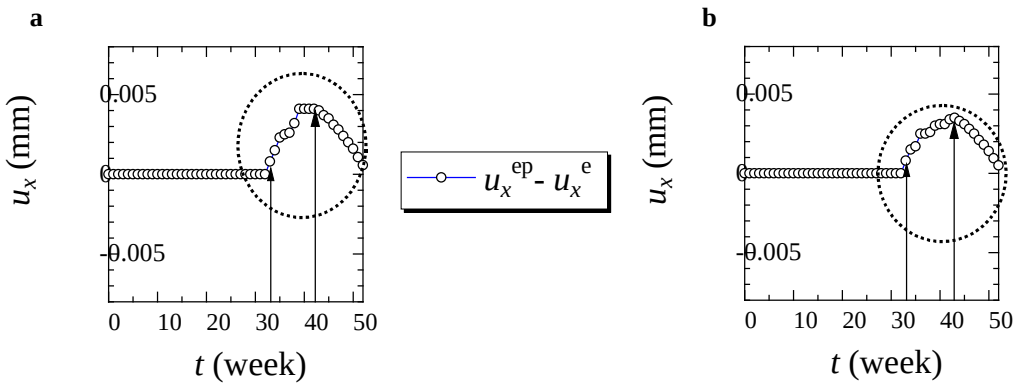


Figure 8. Difference in displacements under analysis: (a) Confined boundary conditions under (7.8–32.2°C) temperature range, (b) confined boundary conditions under (–2.2–22.2°C) temperature range.

Table 1
Properties of rock mass used in the 2-D numerical analyses

| Property | Value |
|---|---|
| Young's modulus, $E$ | 110 (GPa) |
| Poisson's ratio, $\nu$ | 0.2 |
| Uniaxial compression strength, $q_u$ | 181 (MPa) |
| Angle of internal friction, $\phi$ | 30° |
| Friction angle of rupture plane, $\phi'$ | 30° |
| Tensile strength, $T_o$ | 20.4 (MPa) |
| Residual tensile strength, $T_o'$ | 0 (MPa) |
| Heat conductivity, $K$ | 7.40 (W/ m K) |
| Specific heat, $c$ | 995 (J/ kg K) |
| Density, $\rho$ | 2636 (kg/m$^3$) |
| Expansion coefficient | $7.94 \times 10^{-6}$ (K$^{-1}$) |
| Effective porosity, $\eta$ | 0.8% |
| Linear expansion due to freezing | 0.00036 |
| Temperature at which freezing starts | 0°C |
| Temperature at which freezing finishes | -30°C |